

TPR-00-14

# SEMICLASSICAL CALCULATION OF SHELL EFFECTS IN DEFORMED NUCLEI

M. BRACK, CH. AMANN

*Institute for Theoretical Physics, University of Regensburg  
D-93040 Regensburg, Germany*

We summarize recent work in which the shell effect, which causes the onset of the mass asymmetry in nuclear fission, could be explained semiclassically in the framework of the periodic orbit theory. We also present new results for the inclusion of a spin-orbit interaction in the semiclassical calculation of the level density.

## 1 Introduction

The explanation of the asymmetry in the fragment mass distributions of many actinide nuclei has long been a stumbling stone in fission theory. Shortly after the advent of the shell model, Lise Meitner<sup>1</sup> related the mass asymmetry to shell structure, in particular to magic nucleon numbers in one of the fragments. Indeed, since the classical liquid drop model (LDM) prefers symmetric shapes,<sup>2</sup> the mass asymmetry had to be a quantum shell effect. Johansson<sup>3</sup> attempted to calculate fission barriers by summing the single-particle energies of a Nilsson-type shell model including left-right asymmetric deformations. However, due to their wrong average behaviour at large deformations, he could not obtain finite barriers. Only after the introduction of the ingenious *shell-correction method* by Strutinsky<sup>4</sup> this became possible, launching large-scale investigations of the shell structure in fission barriers.<sup>5,6,7</sup> The resulting picture of the *double-humped fission barrier* was nicely confirmed in many detailed experiments.<sup>8</sup>

One interesting outcome was that the *onset* of the left-right asymmetry of the nuclear shapes starts quite early during the fission process: in nuclei like <sup>240</sup>Pu, already the outer fission barrier is unstable against octupole-type deformations.<sup>9</sup> This quantum shell effect could be related to a few specific diabatic single-particle states which were particularly sensitive to the asymmetric deformations.<sup>10</sup> Today, we know that symmetric and asymmetric fission modes may coexist in the same nucleus.<sup>11</sup> Of course, the mass distributions of the fission fragments can only be predicted from a dynamical theory involving inertial parameters.<sup>12</sup> But interestingly enough, the most probable experimental mass ratios were found to be roughly equal to those of the nascent fragments obtained statically at the asymmetric outer barrier.<sup>6,13</sup> The onset of the *mass asymmetry* in nuclear fission was thus established as a *quantum shell effect*

due to specific single-particle states in the deformed average potentials of the nucleons, which could not be understood in the classical liquid drop model.

However, new developments have taken place over the last 25 years to describe quantum shell effects *semiclassically* in the framework of the *periodic orbit theory (POT)*. Through so-called *trace formulae*, the oscillating part  $\delta g(E)$  of the level density of a quantum system can be related to properties of the periodic orbits of the corresponding *classical system*. This approach was systematically developed by Gutzwiller;<sup>14</sup> an alternative derivation valid for billiard systems (i.e., particles enclosed in a cavity with ideally reflecting walls) was given by Balian and Bloch.<sup>15</sup> Strutinsky *et al.*<sup>16,17</sup> generalized the Gutzwiller theory and used it for the semiclassical calculation of shell-correction energies in various shell-model potentials (neglecting, however, the spin-orbit interaction). In particular, they successfully explained the systematics of nuclear ground-state deformations in terms of the leading shortest periodic orbits.<sup>17</sup> Similarly, the onset of the fission mass asymmetry could recently be explained semiclassically.<sup>18</sup> For a comprehensive presentation of the POT, its further refinements, and its applications to various finite fermion systems, we refer to a recent monograph.<sup>19</sup>

In Sect. 2 we summarize the recent work on the fission asymmetry done by one of us (M.B.) in collaboration with P. Meier, S. M. Reimann, and M. Sieber.<sup>18,20,21</sup> In Sect. 3 we present some new semiclassical results for the level density of a three-dimensional deformed potential, including the spin-orbit interaction which so far has been omitted in applications of the POT to the calculation of shell structure in nuclear physics.

## 2 Semiclassical explanation of the onset of mass asymmetry

In our recent semiclassical investigation of the fission mass asymmetry,<sup>18,20</sup> we have approximated the nuclear mean field by a cavity with constant volume and reflecting walls, neglecting the spin-orbit and Coulomb interactions and considering only one kind of particles. We use the parameterization  $(c, h, \alpha)$  of Ref.<sup>6</sup> to define the boundary of the cavity. Here  $2c$  is the length of the nucleus along the symmetry axis (in units of the radius  $R_0$  of the spherical cavity given by  $c=1$ ,  $h=\alpha=0$ ),  $h$  is the neck parameter, and  $\alpha \neq 0$  yields left-right asymmetric shapes. E.g. for  $^{240}\text{Pu}$ , the maximum of the symmetric outer barrier is found<sup>6</sup> near  $c = 1.53$ ,  $h = \alpha = 0$ . Within the POT, the gross-shell effects are given by the shortest periodic orbits of the system. The semiclassical

trace formula for the shell-correction energy  $\delta E$  reads<sup>16,19</sup>

$$\delta E \simeq \sum_{po} \mathcal{A}_{po}(E_F) \left( \frac{\hbar}{T_{po}} \right)^2 \cos \left[ \frac{1}{\hbar} S_{po}(E_F) - \sigma_{po} \frac{\pi}{2} \right]. \quad (1)$$

The sum in (1) is taken over all periodic orbits ( $po$ ).  $S_{po} = \oint_{po} \mathbf{p} \cdot d\mathbf{q}$  are the

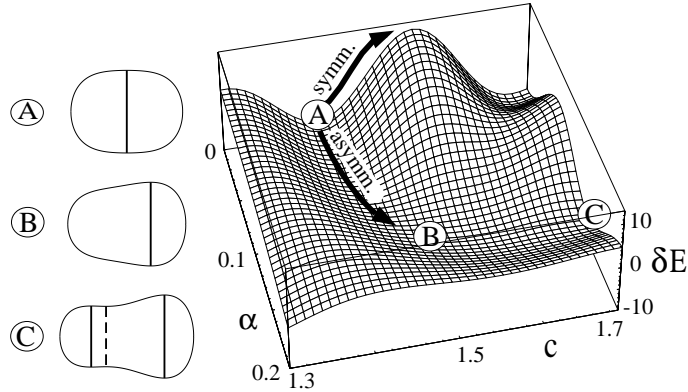


Figure 1: *Right:* Semiclassical deformation energy  $\delta E(c, \alpha)$  ( $\hbar=0$ ) in a perspective 3D plot. The arrows ‘symmetric’ and ‘asymmetric’ show two alternative fission paths. *Left:* shapes along the asymmetric fission path. The planes of the leading periodic orbits are shown by vertical lines (solid for stable and dashed for unstable orbits).

action integrals,  $T_{po} = dS_{po}/dE$  the periods, and  $\sigma_{po}$  are phases related to the number of conjugate points along the periodic orbits. The amplitude  $\mathcal{A}_{po}$  of an orbit depends on its stability and its degeneracy; it includes a factor that exponentially damps contributions from orbits with large periods  $T_{po}$ . All quantities in (1) are evaluated at the Fermi energy  $E_F$ .

In Fig. 1 we show a perspective 3D plot of the deformation energy  $\delta E(c, \alpha)$  ( $\hbar = 0$ ) obtained from Eq. (1). The missing effect of the spin-orbit interaction was compensated by adjusting the only parameter of the model,  $E_F$ , such that the isomer minimum is found at  $c = 1.42$ ,  $\hbar = \alpha = 0$ , corresponding to the quantum result for  $^{240}\text{Pu}$  in the realistic Strutinsky calculations.<sup>6</sup> We see that the semiclassical model correctly yields the instability of the outer barrier against the asymmetry, and a realistic value ( $\sim 0.13$ ) of the parameter  $\alpha$  at the asymmetric saddle point. Inclusion of the LDM energy, which varies very little in the deformation region shown here, does not change this result qualitatively. To the left in Fig. 1 we show the nuclear shapes at three points (A,B,C) along the adiabatic fission path. The vertical lines indicate the planes perpendicular

to the symmetry axis in which the shortest periodic orbits are found. These are simply the polygons with  $p$  reflections inscribed in the circular cross section of the cavity with these planes. A fast convergence of  $\delta E$  with increasing  $p$ , i.e., with the length of the periodic orbits, was found in Ref. <sup>20</sup> ( $p = 2$  and  $3$  were essentially sufficient); other periodic orbits were also shown to be negligible.

We thus obtain a simple physical explanation of the onset of the mass asymmetry of fission in terms of very few classical periodic orbits. The valley of steepest descent through the deformation energy surface is simply given <sup>18</sup> by the requirement that the action of the leading periodic orbits be stationary:  $\delta S_{po} = 0$ . We have also shown <sup>21</sup> that the diabatic states which cause this asymmetry effect quantum-mechanically have their probability maxima exactly on the planes containing the leading periodic orbits, and that a semi-classical quantization of the quasi-regular motion near these planes reproduces the energy levels of the diabatic quantum states surprisingly well.

Our semiclassical picture is only qualitative. It is not meant to replace the Strutinsky (or Hartree-Fock) type calculations, but to give an intuitive physical understanding of the mass asymmetry using classical mechanics. Of course, one has to question if the neglect of the spin-orbit interaction can be justified since it is known to crucially affect the shell structure. Locally, its effect could here be simulated (like in Ref. <sup>17</sup>) by adjusting the Fermi energy. But a semiclassical calculation including spin-orbit effects is certainly desirable.

### 3 Inclusion of spin-orbit interaction in POT

We present now some new results including a spin-orbit interaction in the semiclassical trace formula. The cavity model of the previous section leads to problems with the standard (Thomas) form of the spin-orbit interaction which contains the gradient of the local potential. We therefore use for  $V(\mathbf{r})$  a 3-dimensional deformed harmonic-oscillator potential and add a generalized spin-orbit term which in the spherical limit is proportional to  $\mathbf{l} \cdot \boldsymbol{\sigma}$ :

$$H = \frac{1}{2m} p^2 + V(\mathbf{r}) + \kappa \mathbf{B}(\mathbf{r}, \mathbf{p}) \cdot \boldsymbol{\sigma} \quad (2)$$

with

$$V(\mathbf{r}) = \frac{m}{2} \sum_{i=x,y,z} \omega_i^2 r_i^2, \quad \mathbf{B}(\mathbf{r}, \mathbf{p}) = \nabla V(\mathbf{r}) \times \mathbf{p}. \quad (3)$$

In (2),  $\boldsymbol{\sigma} = (\sigma_x, \sigma_y, \sigma_z)$  are the Pauli matrices. We allow for different frequencies  $\omega_i$  to mimic the shell-model potential of a deformed light nucleus. The quantum-mechanical eigenvalues of (2) were obtained by an exact diagonalization in the basis of  $V(\mathbf{r})$  up to a maximum energy of  $\sim 150 \hbar \omega_x$ .

A first clue to the classical behaviour of this system is gained from a Fourier transform of the oscillating part  $\delta g(E)$  of the level density from the energy to the time domain. To emphasize the gross-shell structure, the level density is Gaussian averaged over an energy range  $\gamma < \hbar\omega_i$ . Due to the energy scaling behaviour<sup>22</sup> of the Hamiltonian (2), the peaks in the Fourier spectrum lie at the time periods  $T_{po}$  of the classical orbits that dominate  $\delta g(E)$ . In Fig. 2 we show the Fourier spectra obtained for a case with *irrational* frequency ratios, both without and with spin-orbit interaction. For  $\kappa = 0$ , we clearly see three

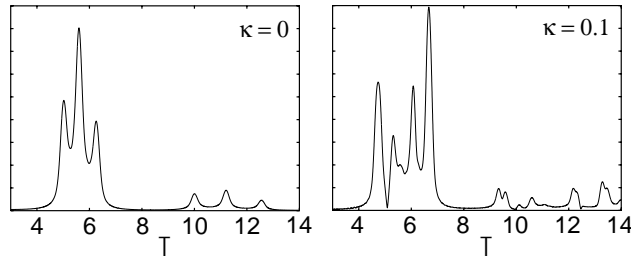


Figure 2: Squared Fourier amplitudes (in arbitrary units) of  $\delta g(E)$  for the anisotropic harmonic oscillator (2) with frequencies  $\omega_x = 1$ ,  $\omega_y = 1.12128$ ,  $\omega_z = 1.25727$ , both without (left) and with spin-orbit interaction (right). Energy eigenvalues up to  $\sim 50 \hbar\omega_x$  were included; the Gaussian averaging range was  $\gamma = 0.2 \hbar\omega_x$ .

main peaks which correspond exactly to the periods  $T_i = 2\pi/\omega_i$  of the only three periodic orbits of this system, which are the librations along the principal axes.<sup>19</sup> At twice these periods, three small peaks corresponding to their second harmonics are visible. For  $\kappa = 0.1$ , a more complicated peak structure is observed, which will be explained in the following.

The problem that arises in the semiclassical description is that the Pauli operators in (2) act on a two-component spinor and couple its components in a non-trivial way. We use the theory of Littlejohn and Flynn,<sup>23</sup> whose basic idea is to diagonalize the Hamiltonian ( $2 \times 2$ ) matrix locally in phase space after its Wigner transformation, and to expand both  $H_W(\mathbf{r}, \mathbf{p})$  and the diagonalizing unitary matrix in powers of  $\hbar$ . Two problems arise in this context. First, on those surfaces in phase space where  $\mathbf{B}(\mathbf{r}, \mathbf{p}) = 0$ , the eigenvalues become degenerate and the method breaks down (so-called *mode conversion*). Second, one obtains gauge-transformation dependencies of the diagonal matrix. This problem can in principle be solved through the introduction of non-canonical coordinates.<sup>23</sup> We will, however, keep the original coordinates and follow the more heuristic method developed by Frisk and Guhr.<sup>24</sup> It leads to the determination of the classical dynamics to lowest order in  $\hbar$  by two classical

Hamiltonian functions  $H_{cl}^{\pm}$

$$H_{cl}^{\pm}(\mathbf{r}, \mathbf{p}) = \frac{1}{2m} p^2 + V(\mathbf{r}) \pm \kappa |\mathbf{B}(\mathbf{r}, \mathbf{p})|, \quad (4)$$

whose combined periodic orbits are to be used in the semiclassical trace formula. The two first-order  $\hbar$  corrections to the energy, denoted by  $\lambda_{Berry}^{\pm}$  and  $\lambda_{NN}^{\pm}$ , may be included perturbatively. Recently, a relativistic trace formula was derived from a semiclassical approximation to the Dirac equation.<sup>25</sup> The same classical Hamiltonians (4) were obtained there in the “large-spin” limit (although the  $\hbar$  corrections were treated differently).

The equations of motion for the Hamiltonians  $H_{cl}^{\pm}$  (4) are

$$\begin{aligned} \dot{r}_i &= p_i \pm \epsilon_{ijk} |\mathbf{B}(\mathbf{r}, \mathbf{p})|^{-1} (B_j \omega_k^2 r_k - B_k \omega_j^2 r_j), \\ \dot{p}_i &= -\omega_i^2 r_i \pm \epsilon_{ijk} |\mathbf{B}(\mathbf{r}, \mathbf{p})|^{-1} (B_j \omega_i^2 p_k - B_k \omega_i^2 p_j). \quad i, j, k \in \{x, y, z\} \end{aligned} \quad (5)$$

This is a non-linear system of six equations, and the search for periodic orbits is not easy. We have determined them by a Newton-Raphson iteration using the stability matrix that is also needed for the amplitudes in the trace formula.<sup>26</sup> Special care must be taken at mode-conversion points where  $\mathbf{B}(\mathbf{r}, \mathbf{p}) = 0$  and hence the right-hand sides of (5) diverge. Some of the periodic orbits, however, can be found more easily. This follows from the fact that the three planes  $r_k = p_k = 0$  ( $k = x, y, z$ ) in phase space are invariant under the Hamiltonian flow. The resulting equations of motion are almost harmonic:

$$\begin{aligned} \dot{r}_i &= p_i \mp \epsilon_{ijk} \text{sign } B_k \omega_j^2 r_j, \\ \dot{p}_i &= -\omega_i^2 r_i \mp \epsilon_{ijk} \text{sign } B_k \omega_i^2 p_j. \quad i, j, k \in \{x, y, z\} \end{aligned} \quad (6)$$

Harmonic solutions of (6) can be obtained analytically by ignoring the factors  $\text{sign } B_k$  that make the system nonlinear, and by accepting only solutions with the correct constant values of  $\text{sign } B_k$ . In total, we find six doubly-degenerate planar solutions with different frequencies  $\omega_{ij}^{\pm}$  ( $i \neq j$ ) given by

$$\tilde{\omega}_{ij}^{\pm} = \left[ \frac{1}{2} \left( \omega_i^2 + \omega_j^2 + 2\kappa^2 \omega_i^2 \omega_j^2 \pm \sqrt{(\omega_i^2 - \omega_j^2)^2 + 8\kappa^2 \omega_i^2 \omega_j^2 (\omega_i^2 + \omega_j^2)} \right) \right]^{1/2}. \quad (7)$$

These solutions all have the form of ellipses, sketched in the left part of Fig. 3, which for  $\kappa \rightarrow 0$  shrink to librations along the  $r_i$  axes with the original frequencies  $\omega_i$ . An important fact for these orbits is that  $B_k \neq 0$  for all  $\kappa \neq 0$ .

It turns out that the frequencies  $\tilde{\omega}_{ij}^{\pm}$ , whose dependence on  $\kappa$  is displayed in the right-hand part of Fig. 3, for  $\kappa = 0.1$  closely agree with the peak positions found in Fig. 2. We cannot resolve all six main peaks; a slightly better resolu-

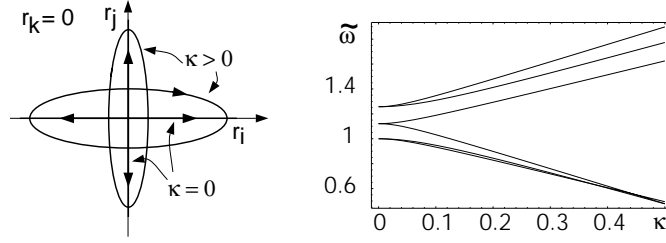


Figure 3: *Left*: A schematic plot of a pair of the 2-dimensional periodic orbits. *Right*: Frequencies  $\tilde{\omega}_{ij}^{\pm}$  (7) of the six planar orbits versus spin-orbit coupling parameter  $\kappa$  (using the same parameters  $\omega_i$  as in Fig. 2.)

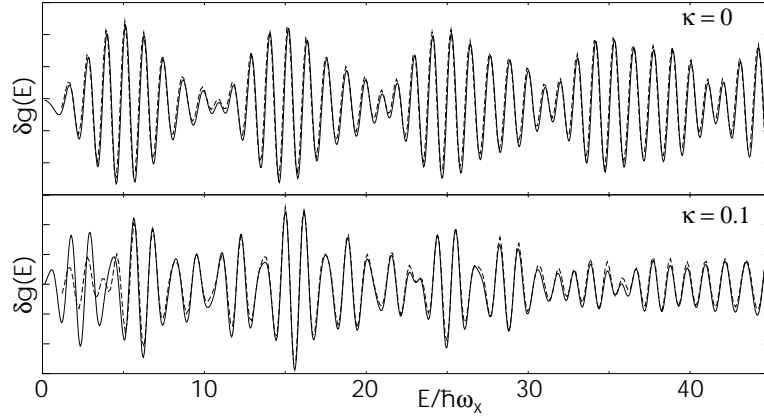


Figure 4: Oscillating part  $\delta g(E)$  of the level density of the 3-dimensional anisotropic harmonic oscillator (same parameters as in Fig. 2, but Gaussian averaging range  $0.5 \hbar \omega$ ). *Solid lines*: quantum-mechanical results; *dotted lines*: semiclassical results, for  $\kappa = 0.1$  using the six planar orbits (first repetitions only) in the trace formula.

tion is found amongst the peaks corresponding to the second harmonics. Some additional small peaks not corresponding to any of the  $\tilde{\omega}_{ij}^{\pm}$  (e.g., the tiny peak at  $T = 10.1$ ) can be explained by genuine three-dimensional orbits.<sup>26</sup>

We now calculate the oscillating part  $\delta g(E)$  of the level density by including the lowest harmonics of the six planar periodic orbits in the trace formula. The  $\hbar$  correction terms for the planar orbits only lead to a constant shift  $\Delta S_{ij}^{\pm} = (\lambda_{Berry} + \lambda_{NN}) T_{ij}^{\pm} = \kappa \pi \omega_k^2 / \tilde{\omega}_{ij}^{\pm}$  of the actions at all energies.<sup>26</sup> The result for  $\delta g(E)$  obtained with  $\kappa = 0.1$  is shown in Fig. 4 by the dotted lines. The quantum-mechanical results are shown by the solid lines. The Gaussian

averaging range was here  $0.5 \hbar \omega_x$  in order to suppress the contributions from second and higher harmonics. For comparison, we also show the curves for  $\kappa = 0$  which exhibit a different shell structure. A good agreement is found also in the presence of the spin-orbit interaction, except for low energies where semiclassical approximations usually are worst. This shows that the planar orbits are the most important ones for the gross-shell structure. The numerical calculation of the three-dimensional orbits and their properties is not difficult as long as they are not crossing the mode-conversion surfaces. A study of their influence on the finer details of the shell structure is in progress.<sup>26</sup>

## Acknowledgment

This work was supported in parts by the Deutsche Forschungsgemeinschaft.

## References

1. L. Meitner, *Nature* **165**, 561 (1950); *Arkiv Fysik* **4**, 383 (1952).
2. see, e.g., S. Cohen and W. J. Swiatecki, *Ann. Phys. (N.Y.)* **19**, 67 (1962).
3. S. A. E. Johansson, *Nucl. Phys.* **22**, 529 (1962).
4. V. M. Strutinsky, *Nucl. Phys. A* **95**, 420 (1967); *ibid. A* **122**, 1 (1968).
5. S. G. Nilsson *et al.*, *Nucl. Phys. A* **131**, 1 (1969).
6. M. Brack *et al.*, *Rev. Mod. Phys.* **44**, 320 (1972).
7. J. R. Nix, *Ann. Rev. Nucl. Sci.* **22**, 65 (1972).
8. For an early review of experimental data on fission barriers, see S. Bjørnholm and J. E. Lynn, *Rev. Mod. Phys.* **52**, 725 (1980); for newer data, see several contributions to this conference.
9. P. Möller and S. G. Nilsson, *Phys. Lett. B* **31**, 283 (1970); H. C. Pauli, T. Ledergerber, and M. Brack, *Phys. Lett. B* **34**, 264 (1971).
10. C. Gustafsson, P. Möller, and S. G. Nilsson, *Phys. Lett. B* **34**, 349 (1971).
11. see, e.g., P. Möller and A. Iwamoto, *Phys. Rev. C* **61**, 047602 (2000); V. V. Pashkevich, this conference.
12. see, e.g., J. Maruhn *et al.*, in *Physics and Chemistry of Fission 1973* (IAEA Vienna, 1974), Vol. I, p. 569.
13. see also W. Greiner *et al.*, this conference.
14. M. C. Gutzwiller, *J. Mat. Phys.* **12**, 343 (1971), and earlier references quoted therein.
15. R. Balian and C. Bloch, *Ann. Phys. (N.Y.)* **69**, 76 (1972).
16. V. M. Strutinsky, *Nucleonica* **20**, 679 (1975); V. M. Strutinsky and A. G. Magner, *Sov. J. Part. Nucl.* **7**, 138 (1976).
17. V. M. Strutinsky *et al.*, *Z. Phys. A* **283**, 269 (1977).



18. M. Brack, S. M. Reimann, and M. Sieber, *Phys. Rev. Lett.* **79**, 1817 (1997).
19. M. Brack and R. K. Bhaduri: *Semiclassical Physics* (Addison and Wesley, Reading, 1997).
20. M. Brack *et al.*, in *Similarities and Differences between Atomic Nuclei and Clusters*, eds. Y. Abe *et al.* (AIP New York, 1998), p. 17.
21. M. Brack, M. Sieber, and S. M. Reimann, in *Nobel Symposium on Quantum Chaos*, ed. K.-F. Berggren; to be published in *Physica Scripta* (2000).
22. Since  $H$  is purely quadratic in the components of  $\mathbf{p}$  and  $\mathbf{r}$ , the classical dynamics governed by Eq. (4) becomes independent of the energy  $E$  after scaling coordinates and momenta by a factor proportional to  $\sqrt{E}$ .
23. G. Littlejohn and W. G. Flynn, *Phys. Rev. A* **44**, 5239 (1991).
24. H. Frisk and T. Guhr, *Ann. Phys. (N.Y.)* **221**, 229 (1993).
25. J. Bolte and S. Keppeler, *J. Phys. A* **32**, 8863 (1999).
26. Ch. Amann and M. Brack, to be published.